Heliyon 10 (2024) e32856

Contents lists available at ScienceDirect

Heliyon

journal homepage: www.cell.com/heliyon

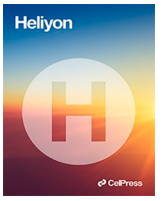

Research article

Forecasting residual mechanical properties of hybrid fibre-reinforced self-compacting concrete (HFR-SCC) exposed to elevated temperatures

Waleed Bin Inqiad [a,*], Elena Valentina Dumitrascu [b], Robert Alexandru Dobre [c,**]

[a] Military College of Engineering (MCE), National University of Science and Technology (NUST), Islamabad, 44000, Pakistan
[b] Computers Department, Faculty of Automatic Control and Computer Science, National University of Science and Technology Politehnica Bucharest, Bucharest, Romania
[c] Electronic Technology and Reliability Department, National University of Science and Technology Politehnica Bucharest, 061071, Bucharest, Romania

ARTICLE INFO

Keywords:
Residual compressive strength
Flexural strength
Fibres
Gene expression programming
Fly ash
Slag
Elevated temperature

ABSTRACT

The use of hybrid fibre-reinforced Self-compacting concrete (HFR-SCC) has escalated recently due to its significant advantages in contrast to normal concrete such as increased ductility, crack resistance, and eliminating the need for compaction etc. The process of determining residual strength properties of HFR-SCC after a fire event requires rigorous experimental work and extensive resources. Thus, this study presents a novel approach to develop equations for reliable prediction of compressive strength (cs) and flexural strength (fs) of HFR-SCC using gene expression programming (GEP) algorithm. The models were developed using data obtained from internationally published literature having eight inputs including water-cement ratio, temperature, fibre content etc. and two output parameters i.e., cs and fs. Also, different statistical error metrices like mean absolute error (MAE), coefficient of determination (R^2) and objective function (OF) etc. were employed to assess the accuracy of developed equations. The error evaluation and external validation both approved the suitability of developed models to predict residual strengths. Also, sensitivity analysis was performed on the equations which revealed that temperature, water-cement ratio, and superplasticizer are some of the main contributors to predict residual compressive and flexural strength.

1. Introduction

Portland cement concrete (PCC) is a globally used construction material and its annual production is more than 25 billion tons. The amount of concrete produced yearly is increasing at the rate of 2.5 % and is expected to reach up to 50 billion tons by 2050 [1]. Cement is the most important ingredient of concrete since it is responsible for binding of all concrete constituents. The production of cement is an energy intensive process which uses naturally occurring materials like limestone etc. and results in huge CO_2 emissions in the atmosphere. In fact, cement industry alone accounts for 7 % of the total CO_2 released in the atmosphere [2]. The yearly production of

* Corresponding author.
** Corresponding author.
E-mail addresses: WaleedBinInqiad@gmail.com (W. Bin Inqiad), elena.dumitrascu97@stud.etti.upb.ro (E.V. Dumitrascu), robert.dobre@upb.ro (R.A. Dobre).

https://doi.org/10.1016/j.heliyon.2024.e32856
Received 21 December 2023; Received in revised form 2 June 2024; Accepted 11 June 2024
Available online 13 June 2024

cement is also expected to go as high as 6000 million tons by 2050. It is reported that production of one ton of cement releases about 900 kg CO_2 in the atmosphere and results in global warming and climate change [3]. Thus, it is imperative to find sustainable alternatives of PCC to reduce the CO_2 emissions in the atmosphere.

Self-compacting Concrete (SCC) has emerged as a viable alternative to ordinary concrete due to its superior properties. It was initially developed in 1980 in Japan but spread throughout the world due to its sustainable advantages. Unlike normal PCC, it flows effortlessly through congested reinforcement cages and members of unconventional geometry. It also compacts itself without the need of mechanical vibrators which are essential for compaction of normal concrete mixtures. It also resists bleeding and segregation during flowing and mixing. The moderate viscosity and low yield stress of SCC mixture ensure optimal compaction without external mechanical intervention. SCC offers many other advantages such as high durability and improved surface finish etc [4]. Due to the transitioning of world towards sustainable solutions, the importance of finding alternative materials for cement in concrete production has also been increased. Industrial by-products like fly ash, ground granulated blast furnace slag, silica fume etc are considered as potential cement and aggregate alternatives because these products have cementitious and pozzolanic characteristics [5–7]. The use of these products in concrete aid in reducing CO_2 emissions and foster a transition towards a sustainable construction industry.

The desirable properties of SCC can only be accomplished with a good mix design because the mixture composition of SCC and quantities of various constituents play a deciding role in achieving segregation resisting and Self-compacting characteristics. The mixture composition of SCC requires the use of greater quantities of finer materials like sand or cement to take up the spaces between coarse aggregate particles making the mixture denser and more durable. Along with the higher level of fines, several chemical admixtures are also important to be added in SCC to make the consistency fluid and make it flow through the formwork [8,9]. Since the utilization of greater quantities of cement in SCC can increase the cost, researchers have advised to use different industrial wastes in place of cement. The addition of these wastes in SCC reduces the cost of SCC, increases durability and workability characteristics, and aligns with the agenda of fostering the use of sustainable building materials and promoting a green and environmentally friendly concrete industry [5,10–13].

1.1. Fibre-reinforced SCC

SCC exhibits a semi-brittle nature like normal concrete and has a tendency to collapse after the appearance of initial few cracks [14]. This property tends to limit its use in the industry [15]. However, SCC can be made ductile by the addition of fibre-reinforcement. The addition of fibres increases strain carrying capacity, fresh and hardened properties and resists the progression of cracks [16]. Steel

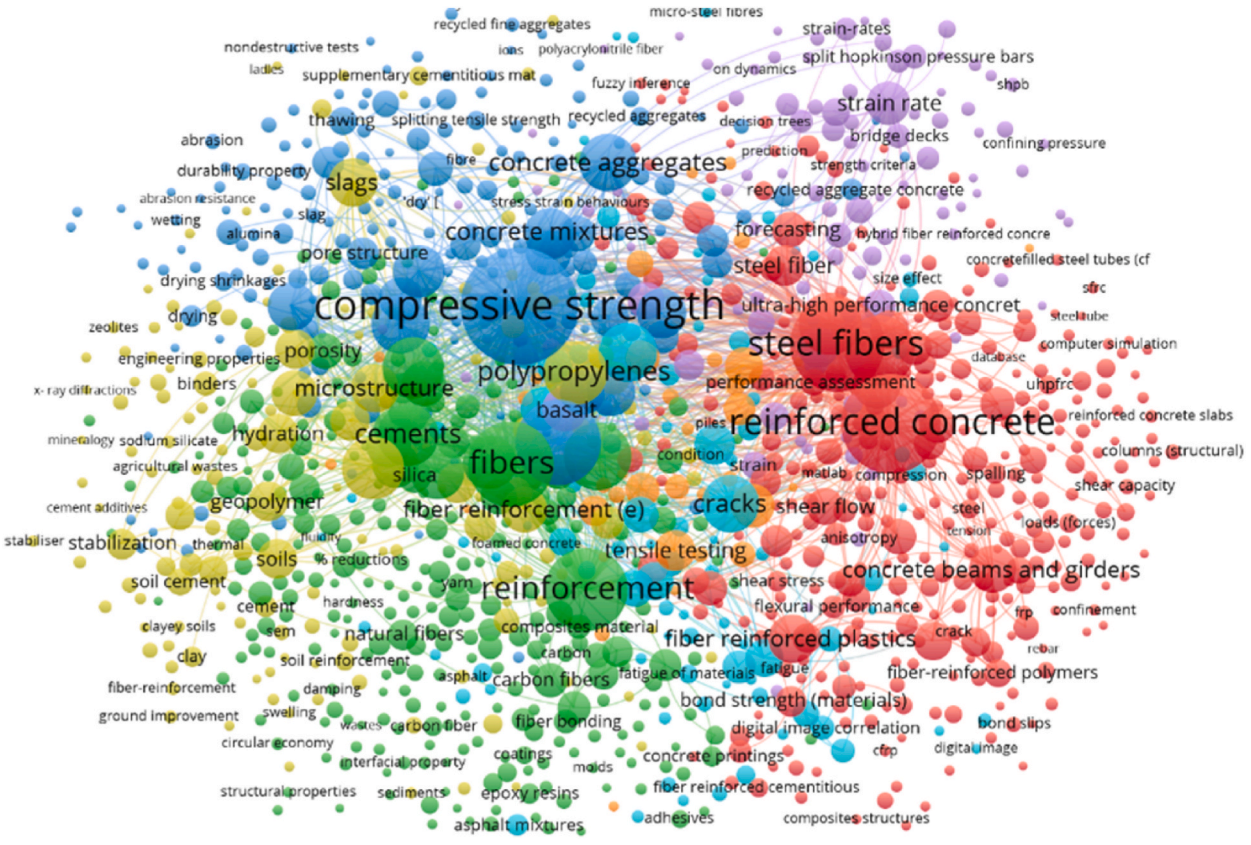

Fig. 1. Scientometric analysis based on the co-occurrence of keywords.

fibres are most commonly used due to their stiffness and cost effectiveness. Synthetic fibres made from polymers are also added in high volumetric ratio due to their immunity against corrosion and low cost compared to steel fibres [17,18]. The randomized arrangement of fibres in the SCC matrix helps in transferring stresses across cracks which leads to an improved post-cracking behaviour of the concrete [19,20]. Many studies also encouraged the use of a mix of different types of fibres in concrete due to their various benefits [21]. The use of fibre-reinforced concrete in precast concrete products, pavements etc and research to study its different properties has been increased recently as shown by the scientometric analysis map shown in Fig. 1. This figure shows the integration of studies related to concrete composites and different types of fibre reinforcement. The map was developed by using the data of last ten years from Scopus database containing keywords "Concrete" and "Fibres". Then, the collected data was analysed using VOSviewer software based on the co-occurrence of keywords. The proportion of articles containing the selected keywords is indicated by the size of the circle and the link between different articles is shown by means of lines between the circles. It can be seen from Fig. 1 that is a plenty of research attributed to using variety of fibres in concrete ranging from steel, polyvinyl, carbon to natural fibres like coconut fibres and measuring mechanical properties like compressive, flexural, and tensile strength of concrete.

1.2. Concrete exposed to elevated temperatures

It is possible that concrete may be exposed to elevated temperatures during its service life. The concrete members in places like factories, chimneys, airport aprons, chemical producing plants are particularly under the risk to be exposed to elevated temperatures. This exposure to high temperature brings about chemical and physical changes in concrete and may result in loss of cs and other mechanical properties of concrete. The behaviour of concrete after exposure to high temperature depends on several factors which include but are not limited to constituents of the concrete itself, maximum temperature it has been exposed to, heating rate, time of exposure, and mechanism adopted to cool the concrete etc [22].

The water present in the pores of concrete evaporates at 105^{o}C, thus the hydrated cement paste dehydrates. Also, gypsum, an ingredient of cement starts to decompose at temperatures of about 110^{o}C–170^{o}C. Another compound $Ca(OH)_2$ present in cement also dehydrates at 400^{o}C and converts to CaO. This conversion liberates the water trapped inside the pores of concrete and results in up to 30 % volume shrinkage accompanied by significant loss of compressive and flexural strengths [23]. Similarly, at temperatures ranging from 180^{o}C to 300^{o}C, the C–S–H compounds commonly called as CSH gel in the hydrated cement paste starts to alter its molecular structure and finally decomposes when temperature reaches 700^{o}C. If the fire is extinguished with water intervention, the CaO formed by the loss of water reacts again with water to form $Ca(OH)_2$ [24]. Also, high temperatures result in heating of aggregates, thermal disconformities in the cement, increase in pore size and porosity etc. This heating and other chemical changes in concrete led to the development of cracks and an undesirable loss of mechanical strength as shown in Fig. 2. HFR-SCC can also be exposed to high temperatures like any other concrete, and it is important to have an estimate of HFR-SCC properties after its exposure to elevated temperatures to make sure that the residual strength of concrete is enough to withstand the loads and the safety of people inhabiting the structure made from HFR-SCC is not compromised.

It is necessary to have a reliable method to compute different mechanical properties of HFR-SCC with a mix of fibres because an accurate estimation of mechanical properties of HFR-SCC is essential to foster its use widely. The strength estimation is of particular importance if the concrete has been subjected to elevated temperatures and there is a risk of reduction in strength of HFR-SCC. The effect of increased temperature on residual mechanical properties of SCC containing steel and synthetic fibres was studied by Sadr-momtazi et al. [25]. The study investigated the effect of temperature ranging from 23^{o}C to 600^{o}C on SCC mixture blended with stone dust. The authors reported that incorporation of steel fibres up to a length of 25 mm resulted in improvement in residual cs and prevented the progression of cracks. Similarly, Eidan et al. [26] studied the influence of length and dosage of fibres on strength of SCC which was exposed to a temperature of 400^{o}C–600^{o}C and concluded that addition of 12 mm long polypropylene fibres resulted in better recovery characteristics.

1.3. Overview of machine learning (ML)

Since there is a transition from analogue to artificial intelligence-based systems in almost every industry, it is no wonder that civil and materials industry is also making its transition towards intelligence-based designs and methodologies driven by data. Artificial intelligence in the realm of civil and structural engineering essentially refers to the amalgamation of advanced ML techniques to optimize construction practices, foster sustainable and intelligent design of infrastructure, and improve the overall efficiency and accuracy of construction industry. ML is a subset of artificial intelligence which enables computers to recognize and learn patterns from the data without explicit guidance from a human and use them to make accurate predictions for future use in return [27]. Deep

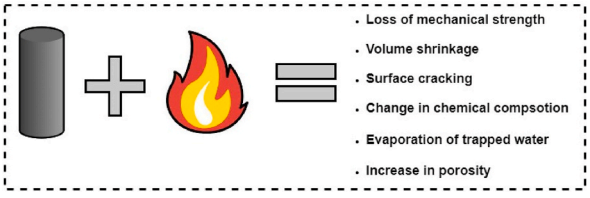

Fig. 2. Effect of increased temperature on concrete.

learning (DL) is in turn a type of ML which involves the use of neural networks to learn patterns from the data. The subtypes of artificial intelligence are shown in Fig. 3. Various ML techniques like artificial neural networks (ANN) etc. are already common in the field of civil engineering. These techniques and several other algorithms are frequently being utilized to estimate different properties of concrete composites, soil compaction parameters, slope failure susceptibility etc [28–40]. This research is attributed to utilization of a special ML algorithm called GEP to predict residual cs and fs of SCC containing a mix of steel, polypropylene and PVA fibres.

2. Relevant literature

In the past few years, the prediction of various properties of concrete composites particularly prediction of strength properties of SCC has been increased. It is due to the shift towards sustainable construction practices and significant benefits of SCC over conventional concrete. For example, in 2021 Farooq et al. [41] conducted a study in which the authors made use of a dataset of 300 points containing industrial waste as a cement replacement in SCC and used Artificial Neural Network (ANN) and Support Vector Machine (SVM) along with GEP to predict cs of SCC. The authors assessed the accuracy by means of error metrices like average error and R^2 and revealed that GEP was the most accurate algorithm to model cs of SCC. Also, the GEP algorithm resulted in a mathematical expression that can be used to predict cs while other two algorithms didn't yield an expression. Similarly, in 2023, Ghunimat et al. [42] leveraged multilayer perceptron (MLP), KNN and radon forest (RF) on an extensive dataset to forecast cs of SCC containing slag and fly ash. The results demonstrated a close resemblance between RF and MLP to accurately predict cs and surpassing KNN. The R^2 value of both MLP and RF was around 0.90 and was 0.81 for KNN. Also, the authors revealed that RF algorithm proved to be resistant to different data splitting combinations and maintained its accuracy unlike the other two algorithms.

In the same way, GEP was utilized by Sonebi et al. to model cs, slump flow and J ring values of pulverized fly ash blended SCC [43]. The GEP model was developed using a small dataset of 26 points to provide empirical expressions for calculation of above-listed properties of SCC. The error evaluation revealed that GEP accurately predicted every SCC property and had R^2 greater than 0.85 for most of the models. The authors also performed a sensitivity analysis on the GEP based equations and concluded that water-to-binder ratio, superplasticizer dosage and quantity of fly ash are some of the main contributors of SCC properties. Moreover, de-Prado-Gil et al. [44] utilized several ML algorithms to predict strength of SCC containing recycled aggregates on an extensive dataset of 515 points. The analysis demonstrated that RF algorithm performed well than all the other regression algorithms and predicted strength values with maximum accuracy and minimal error of 0.712. Also, in a recently conducted study by Mahmood et al. [27], the authors developed SCC by incorporating rice husk ash and marble powder as a replacement of cement. The addition of these waste materials resulted in cost reduction and improvement in different SCC properties. The authors also utilized the laboratory samples to build ML based prediction models for cs of SCC containing fine marble powder and rice husk ash. The authors modelled strength after 90 days of SCC using algorithms such as SVM, KNN, XGB etc. and concluded that all algorithms proved to be accurate to predict cs of SCC with R^2 values greater than 0.9 for most of the cases. The summary of previous related research about the subject of SCC properties prediction is given in Table 1.

Although many studies have been conducted on the subject of predicting strength properties of normal SCC, the area of properties prediction of fibre-reinforced SCC is comparatively unexplored. There are very few studies that report findings about fibre-reinforced SCC strength prediction. The relevant studies include the study conducted by Mai et al. [55], in which the authors assessed different boosting algorithms to predict strength of SCC reinforced with a mix of steel, polypropylene and glass fibres along with different admixtures like marble powder, basalt powder, and limestone etc. The study demonstrated that out of all the boosting algorithms employed, extreme gradient boosting algorithm proved to be the most accurate depicting the least absolute error of 1.43 MPa between real and predicted values. Similarly, Kina et al. [56] utilized deep learning and SVM to estimate cs, fs, and split-tensile strength of SCC

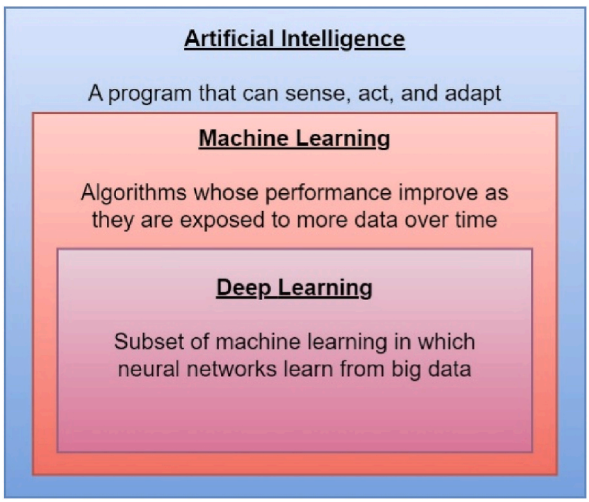

Fig. 3. Artificial Intelligence (AI) and its subtypes.

Table 1
SCC properties prediction by different researchers.

S. No	Machine learning method	Data set	Outputs	Year	Admixtures	References
1.	Neural Networks	111	f_c'	2011	Fly ash Bottom ash	[45]
2.	Inverse Gaussian Extreme Gradient Boosting Extremely Randomized Trees Poisson Gaussian	515	f_c'	2022	Fly ash	[46]
3.	Multivariate adaptive regression splines M5′ algorithm	114	f_c' V-funnel time L-box ratio Slump flow	2018	Fly ash	[47]
4.	Support Vector Machine	327	f_c'	2023	Fly ash	[48]
5.	Genetic Programming	26	f_c' Slump flow J Ring	2009	Fly ash	[49]
6.	Multivariate Regression	63	f_c' Modulus of Elasticity Flexural Strength	2020	Silica fume Crumb rubber	[50]
7.	Artificial Neural Network	114	f_c' Slump flow V-funnel time L-box ratio	2016	Fly ash	[51]
8.	Extreme Learning Machine Long short-term memory	48	Slump flow J Ring	2021	Slag Fly ash Limestone powder Silica fume	[52]
9.	Neural Networks Support Vector Machine	85	f_c'	2022	Fly ash Silica fume	[53]
10.	Multilayer perceptron network Random Forest	1030	f_c'	2022	Fly ash Slag	[42]
11.	Deep Learning Support Vector Regression	24	f_c' Splitting tensile strength	2021	Fly ash Silica fume	[54]

containing a mix of macro steel and micro synthetic fibres. The authors prepared 24 laboratory samples and measured their strength at 7, 28 and 90 days, then utilized that data to build ML models and concluded that deep learning predicted the SCC strength reinforced with different fibres more accurately than SVM. Moreover in 2021, Kina et al. [57] employed deep learning model to forecast fresh and hardened properties of SCC containing a mix of only synthetic fibres. The authors designed 48 SCC mixtures with different proportions of fibres and after measuring their strength and other fresh properties, used that data to create a data-driven model. The developed model predicted every fresh and hardened property of SCC with more than 90 % accuracy. Given that the subject of prediction of fibre-reinforced SCC properties is comparatively unexplored, the studies regarding prediction of residual mechanical properties of HFR-SCC after exposure to elevated temperatures are even more scarce. Thus, this study intends to develop empirical equations for forecasting cs and fs of HFR-SCC.

3. Research significance

As discussed earlier, SCC is a revolutionary concrete composite which has the ability to replace conventional concrete as a sustainable building material. The incorporation of a mix of natural and synthetic fibres can improve the crack resisting properties of SCC and greatly enhance its widespread use. Thus, it is important to have a method for reliably predicting the strength properties of SCC. However, there aren't many studies about properties prediction of HFR-SCC using ML techniques and particularly using genetic programming techniques. Also, it is noteworthy that there exists no study to the best of authors knowledge, which reports the prediction of residual properties of HFR-SCC exposed to elevated temperatures using GEP. Thus, this study is a novel attempt to develop accurate equations to predict cs and fs of HFR-SCC having temperature as an important input parameter. The advantage of using a technique like GEP instead of ANN, RF or XGB is that it represents its output in the form of an empirical equation. The other ML algorithms don't have this ability and thus are frequently categorized as black-box models [58]. In contrast, GEP is a grey-box model because it provides transparency and insight into the prediction process in the form of an empirical relationship between input and output variables [59]. Also, GEP does not call for the need of optimization of a pre-defined model architecture like in ANN etc, thus reducing the time and computing power required to make predictions [60].

4. Gene expression programming (GEP)

John R. Koza introduced genetic programming (GP) for the first time in 1994 [61]. The basic idea of GP revolves around the

amalgamation of natural selection and genetics concept [62]. It utilizes non-linear parse trees in place of binary strings of a pre-defined length and this attribute makes it a useful and versatile instrument to solve mathematical modelling problems. GP makes use of Darwin's theory of evolution and its functioning is very similar to the genetic processes of recombination, mutation, and crossover in humans [61]. It develops models on the basis of genetic evaluation by combining regression and natural selection techniques. These processes help the model to converge to the solution and to remove the sets of least accuracy through the whole evolutionary process [63].

GEP is a sub technique and modification of GP concept based on the evolutionary population algorithm [64]. It outperforms GP because it uses parse trees and fixed length chromosomes. GEP uses genes developed using various arithmetic functions known as primitive functions of fixed lengths to create expression trees (ETs). An ET is basically a non-linear representation of individuals as linear strings having different shapes and sizes but with fixed length [65]. An expression tree contains variables, arithmetic operators, and constant values to represent a mathematical expression. Each ET represent a smaller part of the code which can be combined in various ways to develop the full code containing solution to the problem. The general representation of ET is given in Fig. 4. An ET has different nodes such as root, functional and end nodes as shown in Fig. 4. The expression trees are combined through the genetic processes of mutation and crossover. The visual representation of these processes is given in Fig. 4. These processes result in two offspring which contain the information from their parent. Crossover involves developing a new offspring by combination of two parent trees while mutation means changing an existing parent to get a new offspring [66,67].

The evolution of a computer program to solve the problem on hand begins with creating a randomized set of individuals. These individuals are called chromosomes and the whole set of chromosomes is named as a population. After the population creation, each chromosome is assessed by a pre-determined function called "fitness function" such as average error or R^2. The chromosomes with an acceptable fitness value are selected to be the part of next population while the worst performing chromosomes are removed from the population [62]. This process makes sure that the program eventually converges as close to the real value as possible. This process is repeated many times giving rise to several populations each with a slightly better accuracy then the previous one [68]. This process allows the algorithm to evolve gradually approaching towards the most feasible solution of highest accuracy [43]. The complete sequence of steps followed by GEP algorithm is shown in Fig. 5. The steps outlined in Fig. 4 are repeated over many generations before termination of the algorithm at the most accurate solution.

5. Data collection and analysis

The collection of data to be used for model development is the most crucial step in the development of a ML-based model. Thus, a comprehensive database consisting of 114 data instances for HFR-SCC has been gathered from experimental findings published in international literature [15]. The whole dataset has been divided into training (70 %) and testing (30 %) sets in order to make model accurate to be used on unseen datasets and not overfitted to the training data [69]. This study considers eight input variables and two output variables. The description of these input and output variables along with the statistical description of dataset is given in Table 2.

The distribution of input and output variable(s) is an important factor to consider while collecting data because the performance of

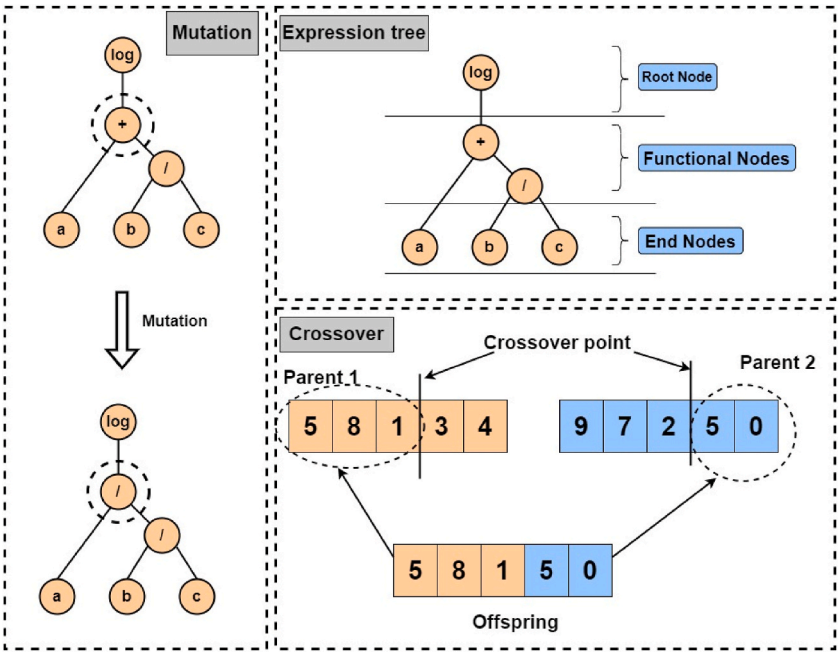

Fig. 4. Representation of expression tree and genetic processes.

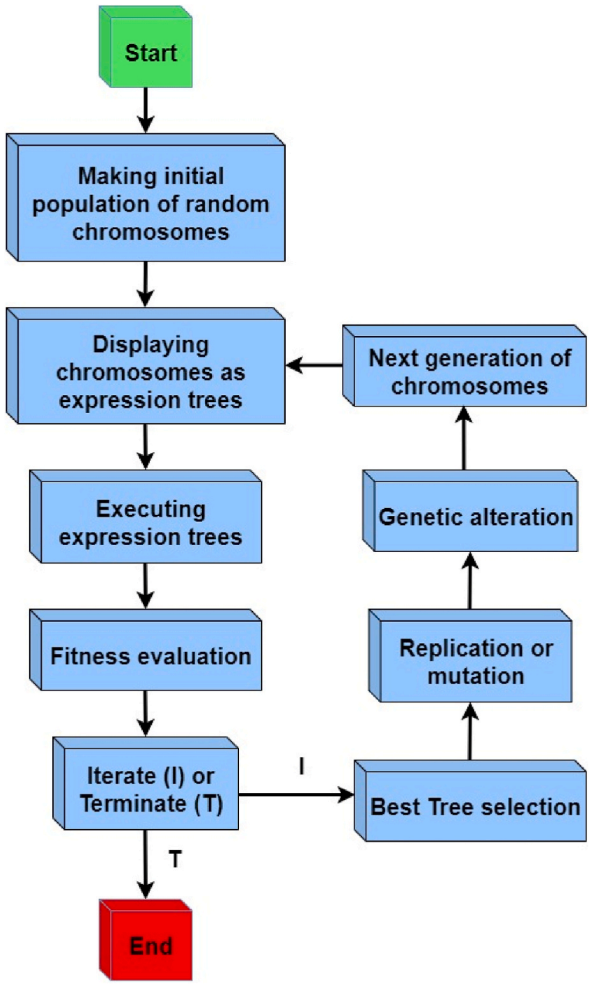

Fig. 5. GEP algorithm flowchart.

a data-driven model depends upon the distribution of explanatory variables. Thus, the contour plots of input variables with both outputs are shown in Fig. 6. Notice from the figure that the input and output variables are spread across a broad range. The contour plots give insight into the variation of output variables with variation in a particular input and the frequency distribution curves at right and above of the contour plots provide information about the distribution of variables. It is evident from contour plots that the output variables are significantly affected by the variation in input variables. These distributions provide a key role in capturing model behaviour and developing a robust model because a model developed using a broader range of data will be more accurate and widely applicable [70].

Table 2
Descriptive analysis of data.

	Units	Symbol	Maximum	Minimum	Mean	Standard Deviation
Water-to-cement ratio	kg/m^3	A	1.08	0.340	0.688	0.354
Fly ash	kg/m^3	B	300	0	126.31	133.73
Slag	kg/m^3	C	292.5	0	128.28	145.78
Fine Aggregate	kg/m^3	D	973.8	756	820.86	85.85
Coarse Aggregate	kg/m^3	E	1143	167.6	720.12	434.21
Superplasticizer	kg/m^3	F	22	7.2	12.02	5.13
Fiber	kg/m^3	G	83.25	0	32.86	37.29
Temperature	^oC	H	900	20	376.31	286.9
Compressive Strength	MPa	cs	103.6	3.84	48.85	27.16
Flexural Strength	MPa	fs	20.98	0.04	5.238	4.28

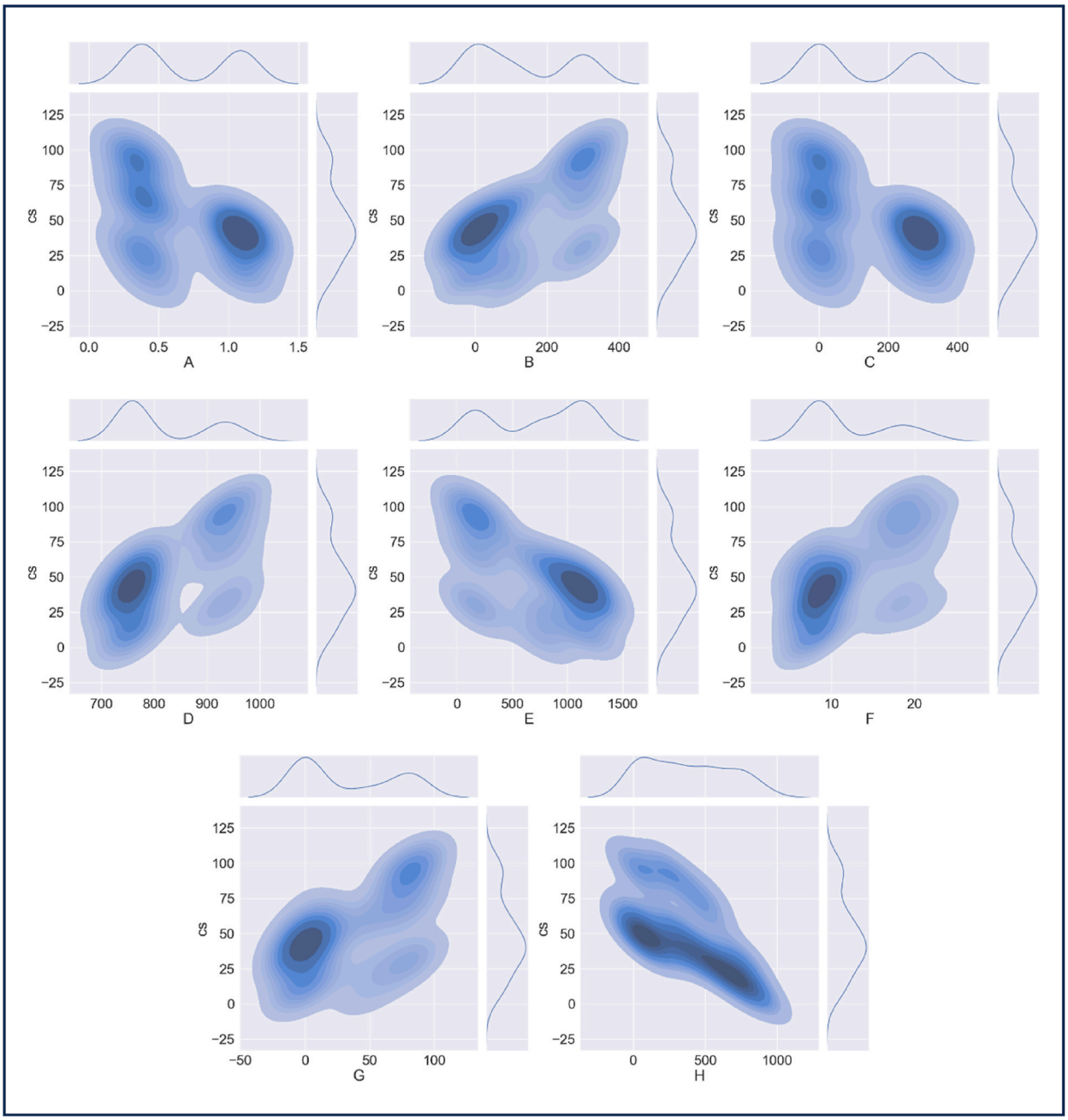

Fig. 6. Contour plots between inputs and outputs.

6. Performance assessment

The developed models using GEP will be checked by means of different error metrices because it is necessary to make sure that the models can effectively solve the given problem without abnormally large errors [71]. The metric R^2 is frequently used as an indicator of model's general accuracy [72]. However, due to its insensitivity towards some conditions such as a constant value being multiplied or divided with the output [73], several other metrices are used alongside it. The metrices MAE and RMSE are described as crucial for evaluating a ML based model [71]. MAE measures average error between real and predicted values and RMSE gives an indication of presence of larger errors [74]. The two metrices performance index (PI) and objective function (OF) are commonly used as indicators of model's overall performance because they simultaneously consider correlation coefficient, relative root mean squared error, and the relative number of data points in both training and testing sets to assign a performance value to the model [75]. Thus, every metric has

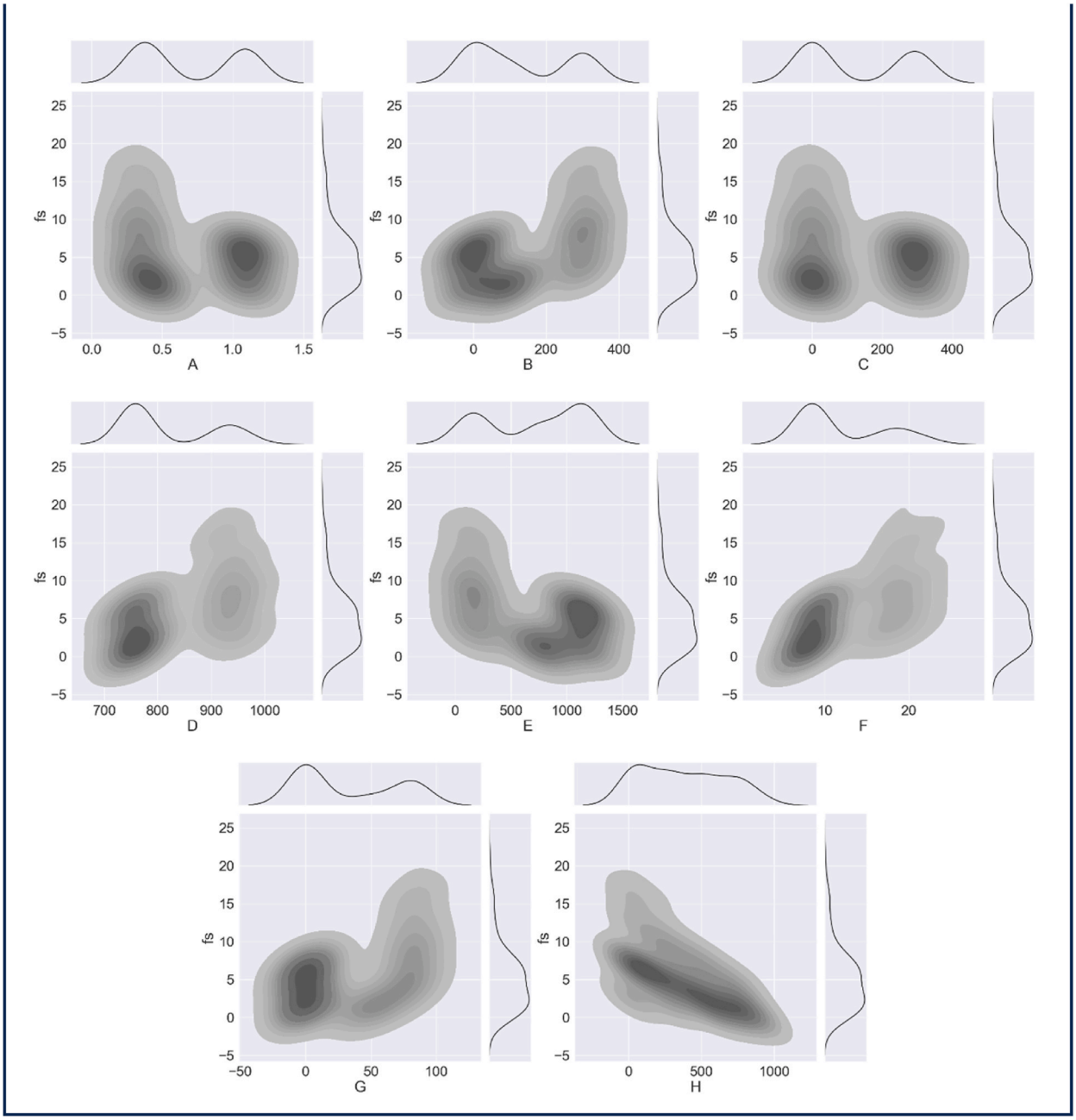

Fig. 6. (*continued*).

its own importance. The employed error metrices, their mathematical formulas, their range and suggested criteria for acceptable models are given in Table 3. The criteria given in Table 3 will be used to check the suitability of the resulting equations by GEP.

7. Results and discussions

7.1. Compressive strength prediction using GEP

The GEP algorithm was employed using a software known as GeneXpro Tools. Before starting the actual model creation process, there are several fitting parameters of GEP algorithm that need to be selected. These parameters were selected using a trial-and-error method in which these parameters were varied across a range of possible values and the combination of parameters which resulted in maximum accuracy were selected. The combination of hyperparameters used for cs prediction process is shown in Table 4. Notice that

Table 3
Summary of error evaluation criteria.

No.	Metric	Abbreviation	Formula	Range	Suggested value
1.	Mean absolute error	MAE	$\frac{\Sigma \lvert x - y \rvert}{n}$	0 to + ∞	Close to zero
2.	Root mean square error	RMSE	$\sqrt{\frac{\sum (x - y)^2}{n}}$	0 to + ∞	Close to zero
3.	Coefficient of determination	R^2	$1 - \frac{\sum (x - y)^2}{\sum (y - y_{mean})^2}$	0 to 1	$R^2 > 0.8$
4.	Performance index	PI	$\frac{RRMSE}{1 + R}$	0 to + ∞	PI < 0.2
5.	Objective Function	OF	$\left(\frac{n_{Training} - n_{Testing}}{n}\right) PI_{Training} + 2\left(\frac{n_{Testing}}{n}\right) PI_{Testing}$	0 to + ∞	OF < 0.2

only simple arithmetic functions are chosen to be included in the final equation as an attempt to keep the resulting equation simple and compact. Also, addition is used as linking function. It means that the sub-expressions resulting from each tree were added to get the final result. These sub-expression trees are shown in Fig. 7 and the resulting equation for computing cs obtained after summation of expressions from each tree is given by Equation (1). The description of variables A,B,C, …etc. used in Equation (1) is given in Table 2. Moreover, the description of constants $C_1, C_2, \ldots$ is also given in Table 5. The prefixes $T_1, T_2, \ldots$ added with the constants specify the tree in which the particular constant is present.

$$cs = T_1 + T_2 + T_3 + T_4 \tag{1}$$

Where.

$$T_1 = \sqrt{D + [D - \{(-8.579 - C + 2H) - 0.327H\}]}$$

$$T_2 = \frac{F}{A} - \left[\frac{\sqrt{H} - \left(\frac{B}{F}\right)}{\sqrt{F.A}}\right]$$

$$T_3 = \left\{\left(\frac{H}{-3.494F}\right)\left(\sqrt{H + H}\right)\right\} + \sqrt{\sqrt{G.B}}$$

$$T_4 = \left(\frac{\sqrt{H.F}}{(H.G) + (H.E)}\right)\left(\frac{-1059.89d_5}{5.483 - B}\right)$$

7.2. Flexural strength prediction using GEP

The flexural strength prediction was also done using the same software as cs. The hyperparameters were also varied across the permissible range before reaching a combination of parameters which led to the most accurate equation. This combination is given in Table 4. The GEP algorithm displayed the result in the form of several expression trees given in Fig. 8. The expression from each tree was linked by the chosen linking function, addition in this case to get the final result given by Equation (2) for residual fs prediction of HFR-SCC. The description of variables involved in equation (2) and constants involved in expression trees is given in Tables 2 and 5 respectively.

$$fs = T_5 + T_6 + T_7 + T_8 \tag{2}$$

$$T_5 = \frac{18.347}{\sqrt{(13.169 + B)}}$$

Table 4
Hyperparameter settings of GEP.

Parameters	Settings	
	cs Prediction	fs Prediction
No. of Chromosomes	30	30
No. of Genes	10	8
Head Size	4	4
Linking Function	Addition	Addition
Constants per Gene	10	10
Functions	+, -, x, ÷, sqrt	+, -, x, ÷, sqrt

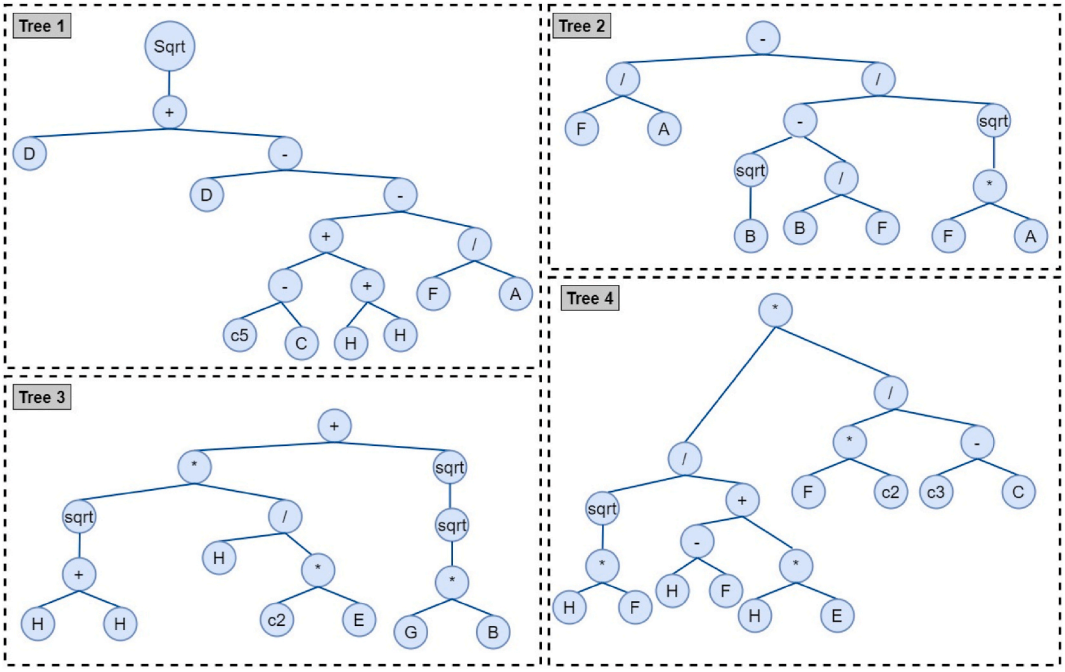

Fig. 7. Expression tree representation of GEP equation to predict compressive strength.

Table 5
Result of error evaluation of developed models.

Name	Value
T_1C_5	−8.579
T_3C_2	−3.49
T_4C_2	−1059.89
T_4C_3	5.48
T_5C_3	5.178
T_5C_9	13.169
T_6C_3	6.034
T_7C_1	2.673

$$T_6 = \frac{d_7}{[G - \{(E + D) - D\}] - 6.034}$$

$$T_7 = F + \frac{H}{[\{(B - G)2.676\} - D] - C}$$

$$T_8 = \sqrt{A}$$

7.3. Error assessment of developed models

The summary of calculated error metrices for training and testing sets used for cs and fs prediction of HFR-SCC by GEP algorithm is given in Table 6. Notice that the R^2 values for both datasets for cs and fs prediction are greater than the permissible value of 0.8 which is an indication of remarkable accuracy of GEP to accurately predict values. The R^2 values are greater for cs prediction than fs. Also, the value of performance index is lower in the case of cs prediction. Moreover, the OF value which is an indication of overall performance of the model is least for cs. It means that GEP algorithm did a good job in predicting residual cs of HFR-SCC rather than fs. But it is noteworthy that the developed model for fs is also accurate with an average error of mere 1.1 MPa. Also, all the other error metrices are within the suggested range for fs prediction as they are for cs prediction. The accuracy of models can also be visualized by means of scatter plots as shown in Fig. 9. The scatter plot of cs prediction is given in Fig. 9 (a) and it can be seen that the points lie close to the ideal fit lines for both training and testing data phases which indicates the accuracy of the algorithm. The linear fit line joins the point where there is a 100 % correlation between actual and predicted values and the closer the points are to the linear fit line, the more accurate the algorithm is, and vice versa. Also, the residual distribution plot is placed above the scatter plot to provide more insights

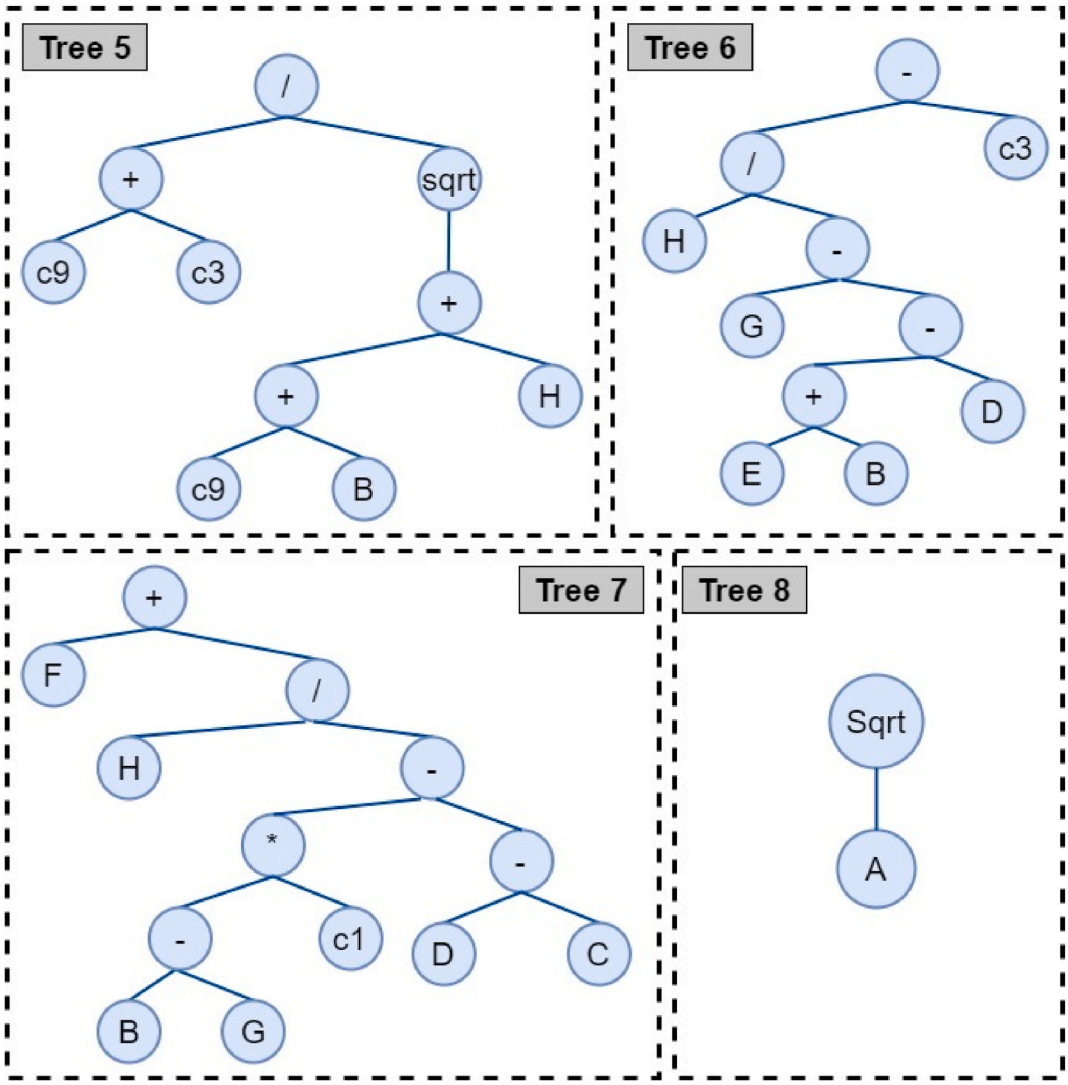

Fig. 8. Expression tree representation of GEP equation to predict flexural strength.

Table 6
Result of error evaluation of developed models.

	cs		fs	
	Training	Validation	Training	Validation
MAE	4.671	4.54	1.07	1.1
RMSE	5.875	5.649	1.37	1.625
R^2	0.952	0.963	0.89	0.90
PI	0.058	0.089	0.139	0.147
OF	0.076		0.154	

into the difference between actual and model predicted values. Residual means the difference between actual, and model predicted values and it is important for highlighting the minimum, maximum, and average difference between the actual and predicted values. Notice from Fig. 9 (a) that most of the residuals lie in the small range of −5 to 5 which shows that GEP does not give large errors in prediction of cs. Similarly, the scatter plot and corresponding residual distribution plot for fs prediction are given in Fig. 9 (b) and notice that the points also lie close to the linear fit line except for a few points. Thus, from the error evaluation summary and scatter plots, it can be inferred that GEP proved to be robust to estimate both residual cs and fs of HFR-SCC.

A common problem which can occur when developing ML models is overfitting. It refers to a condition where a model achieves good accuracy on the training data but doesn't perform well on unseen data [76]. A comparison between the error metrices of training

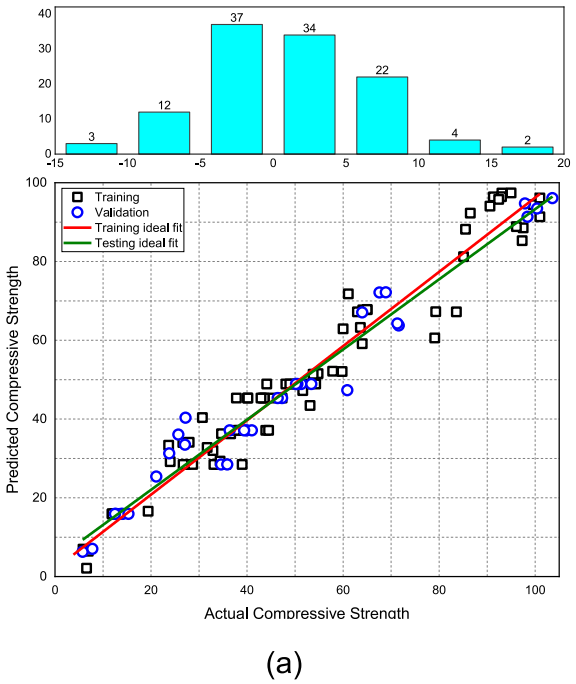

Fig. 9. Scatter plot between actual and predicted values; (a) cs; (b) fs.

and test phase can provide an indication of overfitting. If the error metrices of testing set are significantly greater than those of training set, it indicates that the model is overfitted to the data it is trained on [77] and such model is not suitable to be used practically. Regarding the models developed in current study, it can be seen from Table 6 that the testing error metrices of for both cs and fs prediction are less than the training ones. It means the models maintained their accuracy when used on test data and have good generalization capacity. It further reinforces the robustness of GEP-based equations to accurately predict cs and fs of HFR-SCC.

Although the accuracy of GEP to model fs and cs of HFR-SCC can be compared by using the values of statistical error metrices given in Tables 6 and it is beneficial to have a visual representation of the model's predictions compared to the experimental values. Thus, Fig. 10 represents curve fitting or series plots between real and predicted values for both cs and fs prediction models. These curve

fitting plots prove very useful to visualize the predictive capabilities of the model. It is evident from Fig. 10 that GEP predicted accurate values of both cs and fs at most of the points. However, GEP failed to accurately predict fs at some points and as a result, the difference between actual and predicted values for fs model is large at several points as evidenced by Fig. 10 (b) as compared to the errors in predicting cs in Fig. 10 (a).

7.4. External validation of models

Table 7 provides the summary of some external validation checks applied on the developed equations to independently validate their accuracy. It is evident from Table 7 that the developed equations for fs and cs satisfy all the validation checks. In the table, s or s′ are used as a description of slope of regression lines passing through the origin and their value must lie between 0.85 and 1.15 for a model to be acceptable [78]. Similarly, R_o^2 represents correlation between real and predicted values and it must be closer to 1 [79]. Also, R_m is used to measure the absolute difference between R_o^2 and R^2 [80]. Moreover, the index n is also frequently utilized as an external validation check and its value must be less than 0.1 for a good model [81].

7.5. Sensitivity analysis (SA)

The developed equations for cs and fs prediction of HFR-SCC went under SA to gain further insights about the significance of different input parameters in predicting the output. It is necessary to carry various explanatory analysis on developed ML models because the good performance of a model on training and testing datasets can't be used as a sole indication of model's robustness [82]. The result of SA of both equations are given in Fig. 11. The description of variables $A, B, C, \ldots$ etc is already given in Table 2. It can be seen from Fig. 11 that the residual fs and cs are most affected by the temperature. This is because exposure to elevated temperature results can bring about physical and chemical changes in concrete thus reducing its strength and deteriorating it physically [15]. At temperature of about 105°C, water present in the pores of concrete evaporates, also gypsum present in the cement starts decomposing at temperatures as low as 110°C. Moreover, at temperature ranging from 400°C to 600°C, the $Ca(OH)_2$ dehydrates and converts into CaO, which results in development of shrinkage stains and strength deterioration [83]. Thus, temperature is the most predominant factor in estimation of residual mechanical properties of HFR-SCC. After temperature (51 %), water-to-cement ratio (22.6 %) and superplasticizer (6.2 %) are the important factors in determining cs of HFR-SCC. In a recent study conducted by Pakzad et al. [84], the authors described the profound importance of superplasticizer and water-cement ratio for determining strength of SCC reinforced with different types of fibres. The importance of water-cement ratio has also been highlighted in many other studies and it has been listed as the top contributing factor for cs and fs of SCC [85,86]. Similarly, the importance of fine materials added to SCC mixture including mineral admixtures (fly ash and slag) and fine aggregate has been reported earlier in similar studies [87,88]. Also, Zheng et al. [89] documented the role of fibres after mineral admixtures to predict SCC strength. Moreover, Ahmed et al. [90] reported the

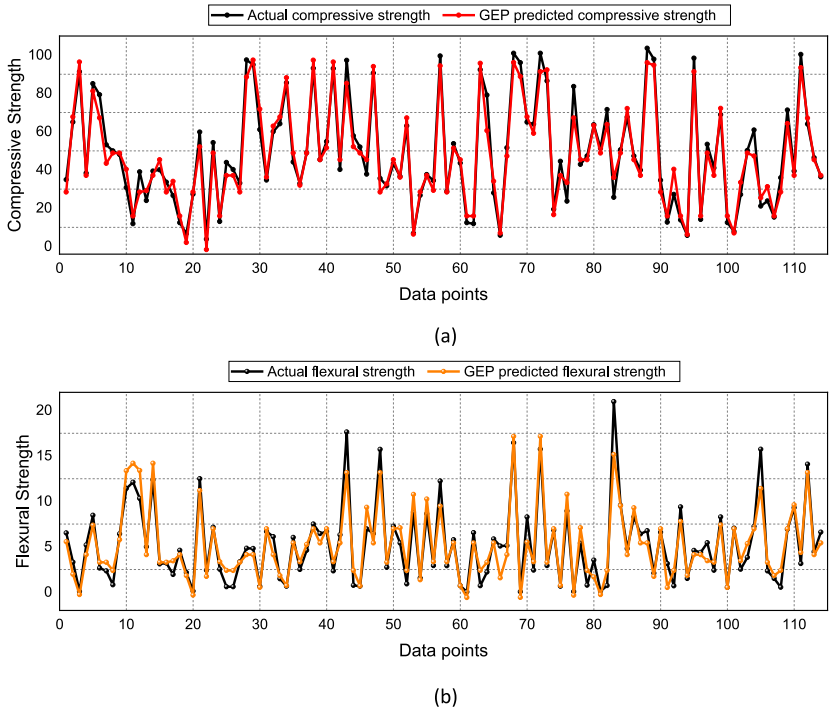

Fig. 10. Series plot of actual and predicted values; (a) compressive strength; (b) flexural strength.

Table 7
External validation checks applied on the models.

Expression	Criteria	cs	fs
$s = \frac{\sum_{i=1}^{n}(x_i \times y_i)}{\sum_{i=1}^{n}(x_i^2)}$	$0.85 < s < 1.15$	0.969	0.941
$s' = \frac{\sum_{i=1}^{n}(x_i \times y)}{\sum_{i=1}^{n}(y_i^2)}$	$0.85 < s' < 1.15$	1.02	1.013
$R_m = R^2 \times \left(1 - \sqrt{\lvert R^2 - R_o^2 \rvert}\right)$	$R_m > 0.5$	0.790	0.58
$R_o^2 = 1 - \frac{\sum_{i=1}^{n}(y_i - x_i^o)^2}{\sum_{i=1}^{n}(y_i - y_i^o)^2}, \quad x_i^o = s \times y_i$	$R_o^2 \approx 1$	0.926	0.999
$R = \frac{(n\sum y - (\sum x)(\sum y))}{\sqrt{\left(n\sum x^2 - (\sum x)^2\right)\left(n\sum y^2 - (\sum y)^2\right)}}$	$R > 0.8$	0.977	0.940
$m = \frac{R^2 - R_o^2}{R_o^2}$	$m < 0.1$	0.03	−0.11

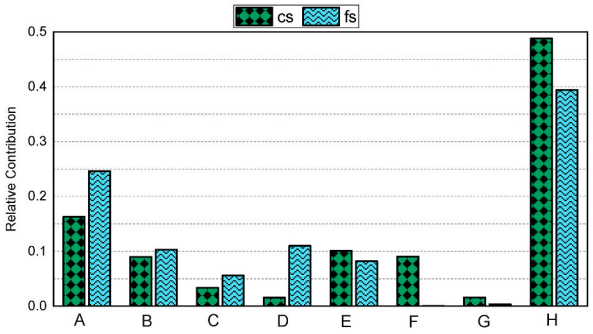

Fig. 11. Relative importance of variables to predict outputs.

comparatively lesser role of coarse aggregate in SCC strength determination. Thus, the result of SA aligns perfectly with the real world and findings of the previously conducted research.

7.6. Practical implications of the study

It is important to highlight the practical implications of such empirical studies to further highlight their importance. It has already been discussed in introduction section that SCC has the potential to replace conventional concrete as a feasible alternative due to its significant advantages and help in transitioning towards sustainable building materials. The incorporation of fibres in SCC can help improve its ductility and post-cracking behaviour. However, the accurate prediction of mechanical properties of HFR-SCC is important to foster its widespread use to make precast concrete products and other applications. In case of a fire event, the members made out of HFR-SCC can suffer a significant loss in mechanical strength and sometimes the structure can collapse if the residual strength is less than the service loads of the structure. Thus, it is important to have an idea of the residual strength of the concrete members to make sure that they can withstand their service loads.

This study was conducted in an attempt to provide empirical equations which can be effectively used by professionals in the fire safety industry to get an idea about the residual mechanical properties of HFR-SCC members after their exposure to elevated temperature. The physical properties of HFR-SCC suffer a significant loss in mechanical properties and change in chemical composition after a fire event, and the equations developed in this study can be used to know whether the structure has sufficient residual strength for safely serving its purpose or not. The use of these equations will escalate the process of determining residual strength by eliminating the need of rigorous experimental work and will aid in quick deployment of remedial measures.

8. Conclusions

This study was conducted to develop accurate equations to predict residual compressive and flexural strength of HFR-SCC exposed to high temperatures using GEP due to the reason that it can represent its output in the form of an empirical equation unlike other black-box ML algorithms. The dataset for HFR-SCC collected from literature had a mix of steel and synthetic polypropylene fibres. The main conclusions of this study are.

- GEP algorithm yielded empirical equations for prediction of both residual properties of HFR-SCC and error evaluation of developed equations revealed that both are accurate, and errors lie within the suggested criteria.
- GEP did a good job in predicting residual cs as evident from a testing R^2 of 0.96 compared to fs prediction whose testing R^2 was equal to 0.90. Similarly, cs prediction equation had an OF value of 0.076 demonstrating the superior overall performance of the model compared to 0.154 value of for fs prediction.
- The developed equations also went under some external validation checks which again approved the robustness of both models.
- Sensitivity analysis was done on both models and the results revealed that temperature is the most significant factor in determining residual cs and fs of HFR-SCC followed by water-to-cement ratio, admixtures, and superplasticizer dosage.

9. Recommendations

Although this study is a significant contribution to the literature about predicting residual strength of HFR-SCC using ML techniques, it is important to highlight its limitations and give suggestions for future research.

- The models presented in this study were developed using a dataset of 114 points taken from already published literature. However, it is important to consider a larger dataset for future studies to develop more robust prediction models.
- Different material properties like nominal aggregate size, average length of incorporated fibres, type of superplasticizer used, and some other properties like time of exposure to high temperature etc. affect the residual properties of SCC. This study does not explicitly incorporate the effect of these factors but recommends considering them in future studies.
- The models in this study were developed using a data whose range is given in Table 2. For the development of more widely applicable models, it is necessary to consider a wider range of data.

Data availability

The data used is provided in the article.

CRediT authorship contribution statement

Waleed Bin Inqiad: Writing – review & editing, Writing – original draft, Visualization, Validation, Software, Methodology, Investigation, Formal analysis, Data curation, Conceptualization. **Elena Valentina Dumitrascu:** Validation, Supervision, Software, Resources, Project administration, Methodology, Investigation. **Robert Alexandru Dobre:** Writing – review & editing, Validation, Supervision, Resources, Project administration, Funding acquisition.

Declaration of competing interest

The authors declare that they have no known competing financial interests or personal relationships that could have appeared to influence the work reported in this paper.

Acknowledgements

This work was supported by a grant from the National Program for Research of the National Association of Technical Universities - GNAC ARUT 2023.

Appendix

Table A
Dataset used for model development.

No.	A kg/m^3	B kg/m^3	C kg/m^3	D kg/m^3	E kg/m^3	F kg/m^3	G kg/m^3	H ^oC	cs MPa	fs MPa
1.	0.444	100	0	764	764	7.2	0	600	21.12	0.54
2.	0.444	100	0	764	764	7.2	2	600	24	0.64
3.	0.444	100	0	764	764	7.2	40	600	23.68	0.67
4.	0.444	100	0	764	764	7.2	55	600	26.65	0.66
5.	0.444	100	0	764	764	7.2	43	600	27.09	0.72
6.	0.444	100	0	764	764	7.2	57	600	27.95	0.67
7.	0.444	100	0	764	764	7.2	0	900	3.84	0.04
8.	0.444	100	0	764	764	7.2	2	900	6.6	0.05

(*continued on next page*)

Table A (*continued*)

No.	A	B	C	D	E	F	G	H	cs	fs
	kg/m^3	kg/m^3	kg/m^3	kg/m^3	kg/m^3	kg/m^3	kg/m^3	^oC	MPa	MPa
9.	0.444	100	0	764	764	7.2	40	900	5.76	0.07
10.	0.444	100	0	764	764	7.2	55	900	5.85	0.1
11.	0.444	100	0	764	764	7.2	43	900	6.93	0.12
12.	0.444	100	0	764	764	7.2	57	900	7.8	0.12
13.	1.085	0	292.5	756	1143	9	0.2	500	33.6	3.22
14.	1.085	0	292.5	756	1143	9	0.3	500	34.9	3.11
15.	1.085	0	292.5	756	1143	9	0.5	500	35.9	2.66
16.	1.085	0	292.5	756	1143	9	0	750	15.3	0.74
17.	1.085	0	292.5	756	1143	9	0	750	11.9	0.6
18.	1.085	0	292.5	756	1143	9	0.1	750	12.4	0.78
19.	1.085	0	292.5	756	1143	9	0.2	750	12.5	0.71
20.	1.085	0	292.5	756	1143	9	0.3	750	11.9	0.6
21.	1.085	0	292.5	756	1143	9	0.5	750	12.7	0.55
22.	1.085	0	292.5	756	1143	9	0.1	750	12.4	0.92
23.	1.085	0	292.5	756	1143	9	0.2	750	13	0.82
24.	1.085	0	292.5	756	1143	9	0.3	750	13.8	0.76
25.	1.085	0	292.5	756	1143	9	0.5	750	14.1	0.72
26.	0.444	100	0	764	764	7.2	0	20	64	2.53
27.	0.444	100	0	764	764	7.2	2	20	60	2.44
28.	0.444	100	0	764	764	7.2	40	20	64	2.51
29.	0.444	100	0	764	764	7.2	55	20	65	2.93
30.	0.444	100	0	764	764	7.2	43	20	63	2.35
31.	0.444	100	0	764	764	7.2	57	20	65	2.91
32.	0.444	100	0	764	764	7.2	0	300	53.12	2.1
33.	0.444	100	0	764	764	7.2	2	300	51.6	2.42
34.	0.444	100	0	764	764	7.2	40	300	53.76	2.16
35.	0.444	100	0	764	764	7.2	55	300	59.8	1.51
36.	0.444	100	0	764	764	7.2	43	300	54.81	1.48
37.	0.444	100	0	764	764	7.2	57	300	57.85	1.52
38.	1.085	0	292.5	756	1143	9	0.1	100	42.9	6.04
39.	1.085	0	292.5	756	1143	9	0.2	100	40.2	6.41
40.	1.085	0	292.5	756	1143	9	0.3	100	40.1	6.62
41.	1.085	0	292.5	756	1143	9	0.5	100	37.8	6.46
42.	1.085	0	292.5	756	1143	9	0.1	100	43.6	6.32
43.	1.085	0	292.5	756	1143	9	0.2	100	45.4	6.46
44.	1.085	0	292.5	756	1143	9	0.3	100	46.4	6.77
45.	1.085	0	292.5	756	1143	9	0.5	100	47.3	6.56
46.	1.085	0	292.5	756	1143	9	0	300	40.2	4.6
47.	1.085	0	292.5	756	1143	9	0	300	39.4	4.44
48.	1.085	0	292.5	756	1143	9	0.1	300	39.4	4.8
49.	1.085	0	292.5	756	1143	9	0.2	300	38.3	4.84
50.	1.085	0	292.5	756	1143	9	0.3	300	37.6	4.62
51.	1.085	0	292.5	756	1143	9	0.5	300	36.4	4.39
52.	1.085	0	292.5	756	1143	9	0.1	300	39.9	5.2
53.	1.085	0	292.5	756	1143	9	0.2	300	41	5.12
54.	1.085	0	292.5	756	1143	9	0.3	300	43.9	5
55.	1.085	0	292.5	756	1143	9	0.5	300	44.5	4.81
56.	1.085	0	292.5	756	1143	9	0	500	39	2.22
57.	1.085	0	292.5	756	1143	9	0	500	35.6	2.35
58.	1.085	0	292.5	756	1143	9	0.1	500	33.1	2.93
59.	1.085	0	292.5	756	1143	9	0.2	500	28.7	2.75
60.	1.085	0	292.5	756	1143	9	0.3	500	27.3	2.42
61.	1.085	0	292.5	756	1143	9	0.5	500	26.7	2.35
62.	1.085	0	292.5	756	1143	9	0.1	500	34.6	3.36
63.	0.34	300	0	949	167.5	19	80	250	101	8.81
64.	0.34	300	0	929.6	164	18	83.25	250	97.5	9.58
65.	0.34	300	0	937.7	165.5	18	82.38	250	96.1	9.31
66.	0.34	300	0	973.8	171.8	15	0	500	60.9	3.16
67.	0.34	300	0	952	168	16	80	500	79.1	6.12
68.	0.34	300	0	918.5	162.1	20	83.25	500	64.1	8.47
69.	0.34	300	0	922.6	162.8	18	82.38	500	63.6	8.28
70.	0.34	300	0	949.5	167.6	19	80	500	79.3	5.42
71.	0.34	300	0	914	161.3	22	83.25	500	68.9	8.28
72.	0.34	300	0	914	161.3	22	82.38	500	67.6	6.97
73.	0.34	300	0	949	167.5	19	80	500	83.6	5.4
74.	0.34	300	0	929.6	164	18	83.25	500	71.6	6.53
75.	0.34	300	0	937.7	165.5	18	82.38	500	71.3	6.41

(*continued on next page*)

Table A (*continued*)

No.	A	B	C	D	E	F	G	H	cs	fs
	kg/m^3	kg/m^3	kg/m^3	kg/m^3	kg/m^3	kg/m^3	kg/m^3	^oC	MPa	MPa
76.	0.34	300	0	973.8	171.8	15	0	750	19.4	1.55
77.	0.34	300	0	952	168	16	80	750	34.4	3.16
78.	0.34	300	0	918.5	162.8	20	83.25	750	25.7	5.45
79.	0.34	300	0	922.6	162.8	18	82.38	750	23.8	5.09
80.	0.34	300	0	949.5	167.6	19	80	750	34.7	2.53
81.	0.34	300	0	914	161.3	22	83.25	750	30.7	4.61
82.	0.34	300	0	914	161.3	22	82.38	750	27.2	3.83
83.	0.34	300	0	949	167.5	19	80	750	36.6	1.95
84.	0.34	300	0	929.6	164	18	83.25	750	32.9	3.54
85.	0.34	300	0	937.7	165.5	18	82.38	750	31.7	3.31
86.	1.085	0	292.5	756	1143	9	0.2	23	54.3	6.6
87.	1.085	0	292.5	756	1143	9	0.3	23	50	6.69
88.	1.085	0	292.5	756	1143	9	0.6	23	50.2	6.69
89.	1.085	0	292.5	756	1143	9	0.2	23	48.9	7.06
90.	1.085	0	292.5	756	1143	9	0.3	23	48.1	7.27
91.	1.085	0	292.5	756	1143	9	0.5	23	44.1	7.15
92.	1.085	0	292.5	756	1143	9	0	23	50.5	6.82
93.	1.085	0	292.5	756	1143	9	0	23	51.3	7.24
94.	1.085	0	292.5	756	1143	9	0	23	52	7.51
95.	1.085	0	292.5	756	1143	9	0.1	23	53.4	6.92
96.	1.085	0	292.5	756	1143	9	0.2	100	47.3	5.86
97.	1.085	0	292.5	756	1143	9	0.3	100	43.3	5.78
98.	0.34	300	0	973.8	171.8	15	0	25	85.1	8.63
99.	0.34	300	0	952	168	16	80	25	100.4	12.49
100.	0.34	300	0	918.5	162.1	20	83.25	25	92.4	20.98
101.	0.34	300	0	922.6	162.8	18	82.38	25	90.6	17.63
102.	0.34	300	0	949.5	167.6	19	80	25	101	12.37
103.	0.34	300	0	914	161.3	22	83.25	25	95	16.44
104.	0.34	300	0	914	161.3	22	82.38	25	93.1	15.74
105.	0.34	300	0	949	167.5	19	80	25	103.6	12.11
106.	0.34	300	0	929.6	164	18	83.25	25	99.6	15.72
107.	0.34	300	0	937.7	165.5	18	82.38	25	97.9	14.1
108.	0.34	300	0	973.8	171.8	15	0	250	61.1	8.28
109.	0.34	300	0	952	168	16	80	250	97.3	9.39
110.	0.34	300	0	918.5	162.1	20	83.25	250	86.5	15.74
111.	0.34	300	0	922.6	162.8	18	82.38	250	85.5	12.24
112.	0.34	300	0	949.5	167.6	19	80	250	98.4	8.94
113.	0.34	300	0	914	161.3	22	83.25	250	93	11.41
114.	0.34	300	0	914	161.3	22	82.38	250	91.3	10.32

Note: The explanation of variables $A, B, C, \ldots$ is given in Table 2.

References

[1] N.C. Onat, M. Kucukvar, Carbon footprint of construction industry: a global review and supply chain analysis, Renew. Sustain. Energy Rev. 124 (May 2020), https://doi.org/10.1016/j.rser.2020.109783.

[2] E. Benhelal, G. Zahedi, E. Shamsaei, A. Bahadori, Global strategies and potentials to curb CO2 emissions in cement industry, J. Clean. Prod. 51 (Jul. 15, 2013) 142–161, https://doi.org/10.1016/j.jclepro.2012.10.049. Elsevier Ltd.

[3] M. Schneider, M. Romer, M. Tschudin, H. Bolio, Sustainable cement production—present and future, Cem Concr Res 41 (7) (Jul. 2011) 642–650, https://doi.org/10.1016/J.CEMCONRES.2011.03.019.

[4] M.M. Kamal, M.A. Safan, A.A. Bashandy, A.M. Khalil, Experimental investigation on the behavior of normal strength and high strength self-curing self-compacting concrete, J. Build. Eng. 16 (Mar. 2018) 79–93, https://doi.org/10.1016/J.JOBE.2017.12.012.

[5] Z. Yang, S. Liu, L. Yu, L. Xu, A comprehensive study on the hardening features and performance of self-compacting concrete with high-volume fly ash and slag, Materials 14 (15) (Aug. 2021), https://doi.org/10.3390/ma14154286.

[6] Y. Jiang, et al., Mechanical properties and acoustic emission characteristics of soft rock with different water contents under dynamic disturbance, International Journal of Coal Science & Technology 11 (1) (May 2024) 1–14, https://doi.org/10.1007/S40789-024-00682-0, 2024 11:1.

[7] S. Wang, J. Guo, Y. Yu, P. Shi, H. Zhang, Quality evaluation of land reclamation in mining area based on remote sensing, Int J Coal Sci Technol 10 (1) (Dec. 2023) 1–10, https://doi.org/10.1007/S40789-023-00601-9/TABLES/6.

[8] P.G. Asteris, K.G. Kolovos, Self-compacting concrete strength prediction using surrogate models, Neural Comput. Appl. 31 (Jan. 2019) 409–424, https://doi.org/10.1007/s00521-017-3007-7.

[9] P.G. Asteris, K.G. Kolovos, M.G. Douvika, K. Roinos, Prediction of self-compacting concrete strength using artificial neural networks, European Journal of Environmental and Civil Engineering 20 (Nov. 2016) s102–s122, https://doi.org/10.1080/19648189.2016.1246693.

[10] A. Kanellopoulos, M.F. Petrou, I. Ioannou, Durability performance of self-compacting concrete, Constr Build Mater 37 (Dec. 2012) 320–325, https://doi.org/10.1016/J.CONBUILDMAT.2012.07.049.

[11] O.M. Ofuyatan, A.G. Adeniyi, J.O. Ighalo, Evaluation of fresh and hardened properties of blended silica fume self-compacting concrete (SCC), Research on Engineering Structures and Materials 7 (2) (Jun. 2021) 211–223, https://doi.org/10.17515/resm2020.228ma1023.

[12] F. Soleimani, G. Si, H. Roshan, J. Zhang, Numerical modelling of gas outburst from coal: a review from control parameters to the initiation process, Int J Coal Sci Technol 10 (1) (Dec. 2023), https://doi.org/10.1007/S40789-023-00657-7.

[13] Z. Ali, M. Karakus, G.D. Nguyen, K. Amrouch, Effect of loading rate and time delay on the tangent modulus method (TMM) in coal and coal measured rocks, Int J Coal Sci Technol 9 (1) (Dec. 2022) 1–13, https://doi.org/10.1007/S40789-022-00552-7/FIGURES/16.

[14] K.B. Ramkumar, P.R. Kannan Rajkumar, K. Gunasekaran, Performance of hybrid steel fiber-reinforced self-compacting concrete RC beam under flexure, Engineering Science and Technology, an International Journal 42 (Jun) (2023), https://doi.org/10.1016/j.jestch.2023.101432.

[15] K. Turk, C. Kina, H. Tanyildizi, E. Balalan, M.L. Nehdi, Machine learning prediction of residual mechanical strength of hybrid-fiber-reinforced self-consolidating concrete exposed to elevated temperature, Fire Technol. 59 (5) (Sep. 2023) 2877–2923, https://doi.org/10.1007/s10694-023-01457-w.

[16] M.M. Hilles, M.M. Ziara, Mechanical behavior of high strength concrete reinforced with glass fiber, Engineering Science and Technology, an International Journal 22 (3) (Jun. 2019) 920–928, https://doi.org/10.1016/J.JESTCH.2019.01.003.

[17] M. Alberti, A. Enfedaque, Optimisation of Fibre Reinforcement with a Combination Strategy and through the Use of Self-Compacting Concrete, J. G.-C. and B., and undefined, Elsevier, 2020 [Online]. Available: https://www.sciencedirect.com/science/article/pii/S0950061819327412. (Accessed 19 December 2023).

[18] J. T.-C. and B. Materials and undefined, Laboratory Evaluation of Self-Compacting Fiber-Reinforced Concrete Modified with Hybrid of Nanomaterials, Elsevier, 2020 [Online]. Available: https://www.sciencedirect.com/science/article/pii/S0950061819326637. (Accessed 19 December 2023).

[19] K.B. Ramkumar, P.R. Kannan Rajkumar, S. Noor Ahmmad, M. Jegan, A review on performance of self-compacting concrete – use of mineral admixtures and steel fibres with artificial neural network Application, Constr Build Mater 261 (Nov) (2020), https://doi.org/10.1016/J.CONBUILDMAT.2020.120215.

[20] C. Sudha, A. Sambasivan, K. Pr, M. J.-E. S. and, and undefined, Investigation on the Performance of Reinforced Concrete Columns Jacketed by Conventional Concrete and Geopolymer Concrete, Elsevier, 2022 [Online]. Available: https://www.sciencedirect.com/science/article/pii/S2215098622001847. (Accessed 1 October 2023).

[21] Z. Wu, K. Henri Khayat, C. Shi, How Do Fiber Shape and Matrix Composition Affect Fiber Pullout Behavior and Flexural Properties of UHPC?, 2018.

[22] D.N. Crook, M.J. Murray, Regain of strength after firing of concrete, Mag. Concr. Res. 22 (72) (Sep. 1970) 149–154, https://doi.org/10.1680/MACR.1970.22.72.149.

[23] O. Dülenci, T. Haktanir, F. Altun, Experimental research for the effect of high temperature on the mechanical properties of steel fiber-reinforced concrete, Constr Build Mater 75 (Jan. 2015) 82–88, https://doi.org/10.1016/j.conbuildmat.2014.11.005.

[24] F.C. Lea, The resistance to fire of concrete and reinforced concrete, Journal of the Society of Chemical Industry 41 (18) (Sep. 1922), https://doi.org/10.1002/JCTB.5000411814.

[25] A. Sadrmomtazi, S.H. Gashti, B. Tahmouresi, Residual strength and microstructure of fiber reinforced self-compacting concrete exposed to high temperatures, Constr Build Mater 230 (Jan) (2020), https://doi.org/10.1016/J.CONBUILDMAT.2019.116969.

[26] J. Eidan, I. Rasoolan, A. Rezaeian, D. Poorveis, Residual mechanical properties of polypropylene fiber-reinforced concrete after heating, Constr Build Mater 198 (Feb. 2019) 195–206, https://doi.org/10.1016/j.conbuildmat.2018.11.209.

[27] M.S. Mahmood, et al., Enhancing compressive strength prediction in self-compacting concrete using machine learning and deep learning techniques with incorporation of rice husk ash and marble powder, Case Stud. Constr. Mater. 19 (Dec. 2023), https://doi.org/10.1016/j.cscm.2023.e02557.

[28] W. Bin Inqiad, M.S. Siddique, S.S. Alarifi, M.J. Butt, T. Najeh, Y. Gamil, Comparative analysis of various machine learning algorithms to predict 28-day compressive strength of Self-compacting concrete, Heliyon 9 (11) (Nov. 2023) e22036, https://doi.org/10.1016/j.heliyon.2023.e22036.

[29] A. Memarzadeh, A.A. Shahmansouri, K. Poologanathan, A novel prediction model for post-fire elastic modulus of circular recycled aggregate concrete-filled steel tubular stub columns, Steel Compos. Struct. 44 (3) (Aug. 2022) 309–324, https://doi.org/10.12989/SCS.2022.44.3.309.

[30] C. Zhang, P. Wang, E. Wang, D. Chen, C. Li, Characteristics of coal resources in China and statistical analysis and preventive measures for coal mine accidents, Int J Coal Sci Technol 10 (1) (Dec. 2023) 1–13, https://doi.org/10.1007/S40789-023-00582-9/FIGURES/13.

[31] M. Wang, X. Xi, Q. Guo, J. Pan, M. Cai, S. Yang, Sulfate diffusion in coal pillar: experimental data and prediction model, Int J Coal Sci Technol 10 (1) (Dec. 2023) 1–12, https://doi.org/10.1007/S40789-023-00575-8/FIGURES/12.

[32] Q. Qi, X. Yue, X. Duo, Z. Xu, Z. Li, Spatial prediction of soil organic carbon in coal mining subsidence areas based on RBF neural network, Int J Coal Sci Technol 10 (1) (Dec. 2023) 1–13, https://doi.org/10.1007/S40789-023-00588-3/TABLES/4.

[33] S. Thiruchittampalam, S.K. Singh, B.P. Banerjee, N.F. Glenn, S. Raval, Spoil characterisation using UAV-based optical remote sensing in coal mine dumps, Int J Coal Sci Technol 10 (1) (Dec. 2023), https://doi.org/10.1007/S40789-023-00622-4.

[34] L. Wang, et al., Effect of long reaction distance on gas composition from organic-rich shale pyrolysis under high-temperature steam environment, Int J Coal Sci Technol 11 (1) (Dec. 2024) 1–18, https://doi.org/10.1007/S40789-024-00689-7/TABLES/2.

[35] L. Sun, M. Li, A. Abdelaziz, X. Tang, Q. Liu, G. Grasselli, An efficient 3D cell-based discrete fracture-matrix flow model for digitally captured fracture networks, Int J Coal Sci Technol 10 (1) (Dec. 2023), https://doi.org/10.1007/S40789-023-00625-1.

[36] G. Yang, Y. Chen, X. Liu, R. Yang, Y. Zhang, J. Zhang, Stability analysis of a slope containing water-sensitive mudstone considering different rainfall conditions at an open-pit mine, Int J Coal Sci Technol 10 (1) (Dec. 2023), https://doi.org/10.1007/S40789-023-00619-Z.

[37] D. Ma, H. Duan, J. Zhang, H. Bai, A state-of-the-art review on rock seepage mechanism of water inrush disaster in coal mines, International Journal of Coal Science & Technology 9 (1) (Jul. 2022) 1–28, https://doi.org/10.1007/S40789-022-00525-W, 2022 9:1.

[38] H. Zheng, B. Jiang, H. Wang, Y. Zheng, Experimental and numerical simulation study on forced ventilation and dust removal of coal mine heading surface, Int J Coal Sci Technol 11 (1) (Dec. 2024) 1–17, https://doi.org/10.1007/S40789-024-00667-Z/FIGURES/20.

[39] Y. Liu, et al., Time-shift effect of spontaneous combustion characteristics and microstructure difference of dry-soaked coal, Int J Coal Sci Technol 10 (1) (Dec. 2023), https://doi.org/10.1007/S40789-023-00616-2.

[40] W. Bin Inqiad, et al., Comparison of boosting and genetic programming techniques for prediction of tensile strain capacity of Engineered Cementitious Composites (ECC), Mater. Today Commun. 39 (Jun. 2024) 109222, https://doi.org/10.1016/j.mtcomm.2024.109222.

[41] F. Farooq, et al., A comparative study for the prediction of the compressive strength of self-compacting concrete modified with fly ash, Materials 14 (17) (Sep. 2021), https://doi.org/10.3390/ma14174934.

[42] D. Ghunimat, A.E. Alzoubi, A. Alzboon, S. Hanandeh, Prediction of concrete compressive strength with GGBFS and fly ash using multilayer perceptron algorithm, random forest regression and k-nearest neighbor regression, Asian Journal of Civil Engineering 24 (1) (Jan. 2023) 169–177, https://doi.org/10.1007/s42107-022-00495-z.

[43] M. Sonebi, A. Cevik, Genetic programming based formulation for fresh and hardened properties of self-compacting concrete containing pulverised fuel ash, Constr Build Mater 23 (7) (Jul. 2009) 2614–2622, https://doi.org/10.1016/j.conbuildmat.2009.02.012.

[44] J. de-Prado-Gil, C. Palencia, N. Silva-Monteiro, R. Martínez-García, To predict the compressive strength of self compacting concrete with recycled aggregates utilizing ensemble machine learning models, Case Stud. Constr. Mater. 16 (Jun) (2022), https://doi.org/10.1016/j.cscm.2022.e01046.

[45] R. Siddique, P. Aggarwal, Y. Aggarwal, Prediction of compressive strength of self-compacting concrete containing bottom ash using artificial neural networks, Adv. Eng. Software 42 (10) (2011) 780–786, https://doi.org/10.1016/j.advengsoft.2011.05.016.

[46] J. de-Prado-Gil, C. Palencia, N. Silva-Monteiro, R. Martínez-García, To predict the compressive strength of self compacting concrete with recycled aggregates utilizing ensemble machine learning models, Case Stud. Constr. Mater. 16 (Jun) (2022), https://doi.org/10.1016/j.cscm.2022.e01046.

[47] A. Kaveh, T. Bakhshpoori, S.M. Hamze-Ziabari, M5' and mars based prediction models for properties of selfcompacting concrete containing fly ash, Period. Polytech. Civ. Eng. 62 (2) (Mar. 2018) 281–294, https://doi.org/10.3311/PPci.10799.

[48] J. Web, L. Chen, and W. Jiang, "Advanced in Engineering and Intelligence Systems Estimation of the Compressive Strength of Self-Compacting Concrete (SCC) by a Machine Learning Technique Coupling with Novel Optimization Algorithms.".

[49] M. Sonebi, A. Cevik, Genetic programming based formulation for fresh and hardened properties of self-compacting concrete containing pulverised fuel ash, Constr Build Mater 23 (7) (Jul. 2009) 2614–2622, https://doi.org/10.1016/j.conbuildmat.2009.02.012.

[50] R. Bušić, M. Benšić, I. Miličević, K. Strukar, Prediction models for the mechanical properties of self-compacting concrete with recycled rubber and silica fume, Materials 13 (8) (Apr. 2020), https://doi.org/10.3390/MA13081821.

[51] O. Belalia Douma, B. Boukhatem, M. Ghrici, A. Tagnit-Hamou, Prediction of properties of self-compacting concrete containing fly ash using artificial neural network, Neural Comput. Appl. 28 (Dec. 2017) 707–718, https://doi.org/10.1007/s00521-016-2368-7.
[52] G. Wang, et al., Research and practice of intelligent coal mine technology systems in China, Int J Coal Sci Technol 9 (1) (Dec. 2022) 1–17, https://doi.org/10.1007/S40789-022-00491-3/FIGURES/13.
[53] N. Abunassar, M. Alas, S.I.A. Ali, Prediction of compressive strength in self-compacting concrete containing fly ash and silica fume using ANN and SVM, Arab J Sci Eng 48 (4) (Apr. 2023) 5171–5184, https://doi.org/10.1007/s13369-022-07359-3.
[54] F. Saberi, M. Hosseini-Barzi, Effect of thermal maturation and organic matter content on oil shale fracturing, Int J Coal Sci Technol 11 (1) (Dec. 2024) 1–19, https://doi.org/10.1007/S40789-024-00666-0/FIGURES/16.
[55] H.V.T. Mai, M.H. Nguyen, H.B. Ly, Development of machine learning methods to predict the compressive strength of fiber-reinforced self-compacting concrete and sensitivity analysis, Constr Build Mater 367 (Feb) (2023), https://doi.org/10.1016/j.conbuildmat.2023.130339.
[56] C. Kina, K. Turk, H. Tanyildizi, Estimation of strengths of hybrid FR-SCC by using deep-learning and support vector regression models, Struct. Concr. 23 (5) (Oct. 2022) 3313–3330, https://doi.org/10.1002/suco.202100622.
[57] C. Kina, K. Turk, E. Atalay, I. Donmez, H. Tanyildizi, Comparison of extreme learning machine and deep learning model in the estimation of the fresh properties of hybrid fiber-reinforced SCC, Neural Comput. Appl. 33 (18) (Sep. 2021) 11641–11659, https://doi.org/10.1007/s00521-021-05836-8.
[58] M. Shahin, M.B. Jaksa, H.R. Maier, Physical modeling of rolling dynamic compaction view project artificial neural networks-pile capacity prediction view project [Online]. Available: https://www.researchgate.net/publication/228364758, 2008.
[59] M. Zare Naghadehi, M. Samaei, M. Ranjbarnia, V. Nourani, State-of-the-art predictive modeling of TBM performance in changing geological conditions through gene expression programming, Measurement 126 (Oct. 2018) 46–57, https://doi.org/10.1016/j.measurement.2018.05.049.
[60] M.A. Khan, A. Zafar, A. Akbar, M.F. Javed, A. Mosavi, Application of gene expression programming (GEP) for the prediction of compressive strength of geopolymer concrete, Materials 14 (5) (Mar. 2021) 1–23, https://doi.org/10.3390/ma14051106.
[61] J. R. Koza and R. Poli, "Chapter 5 GENETIC PROGRAMMING.".
[62] A. Gholampour, A.H. Gandomi, T. Ozbakkaloglu, New formulations for mechanical properties of recycled aggregate concrete using gene expression programming, Constr Build Mater 130 (Jan. 2017) 122–145, https://doi.org/10.1016/j.conbuildmat.2016.10.114.
[63] J. R. Koza and M. Jacks Hall, "SURVEY OF GENETIC ALGORITHMS AND GENETIC PROGRAMMING." [Online]. Available: http://www-cs-faculty.stanford.edu/~koza/.
[64] F. Althoey, et al., Crack width prediction of self-healing engineered cementitious composite using multi-expression programming, J. Mater. Res. Technol. 24 (May 2023) 918–927, https://doi.org/10.1016/j.jmrt.2023.03.036.
[65] A. Ahmad, et al., Prediction of compressive strength of fly ash based concrete using individual and ensemble algorithm, Materials 14 (4) (Feb. 2021) 1–21, https://doi.org/10.3390/ma14040794.
[66] S.M. Mousavi, A.H. Alavi, A.H. Gandomi, M.A. Esmaeili, M. Gandomi, A Data Mining Approach to Compressive Strength of CFRP-Confined Concrete Cylinders, 2010.
[67] Z. Yao, Y. Wang, J. Shen, Y. Niu, J.F. Yang, X. Wei, Synergistic CO2 mineralization using coal fly ash and red mud as a composite system, International Journal of Coal Science & Technology 11 (1) (May 2024) 1–10, https://doi.org/10.1007/S40789-024-00672-2, 2024 11:1.
[68] Z. Shahab, et al., Experimental investigation and predictive modeling of compressive strength and electrical resistivity of graphene nanoplatelets modified concrete, Mater. Today Commun. 38 (Mar. 2024) 107639, https://doi.org/10.1016/j.mtcomm.2023.107639.
[69] A.H. Gandomi, A.H. Alavi, M. Mousavi, S.M. Tabatabaei, A hybrid computational approach to derive new ground-motion prediction equations, Eng. Appl. Artif. Intell. 24 (4) (Jun. 2011) 717–732, https://doi.org/10.1016/j.engappai.2011.01.005.
[70] M.A. Khan, et al., Geopolymer concrete compressive strength via artificial neural network, adaptive neuro fuzzy interface system, and gene expression programming with K-fold cross validation, Front Mater 8 (May 2021), https://doi.org/10.3389/fmats.2021.621163.
[71] A. Rostami, A. Raef, A. Kamari, M.W. Totten, M. Abdelwahhab, E. Panacharoensawad, Rigorous framework determining residual gas saturations during spontaneous and forced imbibition using gene expression programming, J. Nat. Gas Sci. Eng. 84 (Dec. 2020), https://doi.org/10.1016/J.JNGSE.2020.103644.
[72] A.H. Alavi, A.H. Gandomi, M.G. Sahab, M. Gandomi, Multi expression programming: a new approach to formulation of soil classification, Eng. Comput. 26 (2) (Apr. 2010) 111–118, https://doi.org/10.1007/s00366-009-0140-7.
[73] F.E. Jalal, Y. Xu, M. Iqbal, M.F. Javed, B. Jamhiri, Predictive modeling of swell-strength of expansive soils using artificial intelligence approaches: ANN, ANFIS and GEP, J Environ Manage 289 (Jul) (2021), https://doi.org/10.1016/j.jenvman.2021.112420.
[74] M. Despotovic, V. Nedic, D. Despotovic, S. Cvetanovic, Evaluation of empirical models for predicting monthly mean horizontal diffuse solar radiation, Renew. Sustain. Energy Rev. 56 (Apr. 2016) 246–260, https://doi.org/10.1016/J.RSER.2015.11.058.
[75] A.H. Gandomi, D.A. Roke, Assessment of artificial neural network and genetic programming as predictive tools, Adv. Eng. Software 88 (Jun. 2015) 63–72, https://doi.org/10.1016/j.advengsoft.2015.05.007.
[76] X. Fang, B. Tan, H. Wang, Comparative study on the flame retardancy of CO2 and N2 during coal adiabatic oxidation process, Int J Coal Sci Technol 10 (1) (Dec. 2023), https://doi.org/10.1007/S40789-023-00652-Y.
[77] S. Whiteson, B. Tanner, M. E. Taylor, and P. Stone, "Protecting against Evaluation Overfitting in Empirical Reinforcement Learning.".
[78] P.P. Roy, K. Roy, On some aspects of variable selection for partial least squares regression models, QSAR Comb. Sci. 27 (3) (Mar. 2008) 302–313, https://doi.org/10.1002/QSAR.200710043.
[79] H.H. Chu, et al., Sustainable use of fly-ash: use of gene-expression programming (GEP) and multi-expression programming (MEP) for forecasting the compressive strength geopolymer concrete, Ain Shams Eng. J. 12 (4) (Dec. 2021) 3603–3617, https://doi.org/10.1016/j.asej.2021.03.018.
[80] M.A. Khan, A. Zafar, A. Akbar, M.F. Javed, A. Mosavi, Application of gene expression programming (GEP) for the prediction of compressive strength of geopolymer concrete, Materials 14 (5) (Mar. 2021) 1–23, https://doi.org/10.3390/ma14051106.
[81] S. Nazar, et al., Machine learning interpretable-prediction models to evaluate the slump and strength of fly ash-based geopolymer, J. Mater. Res. Technol. 24 (May 2023) 100–124, https://doi.org/10.1016/j.jmrt.2023.02.180.
[82] M.F. Iqbal, et al., Sustainable utilization of foundry waste: forecasting mechanical properties of foundry sand based concrete using multi-expression programming, Sci. Total Environ. 780 (Aug) (2021), https://doi.org/10.1016/j.scitotenv.2021.146524.
[83] O. Dülenci, T. Haktanir, F. Altun, Experimental research for the effect of high temperature on the mechanical properties of steel fiber-reinforced concrete, Constr Build Mater 75 (Jan. 2015) 82–88, https://doi.org/10.1016/j.conbuildmat.2014.11.005.
[84] S.S. Pakzad, N. Roshan, M. Ghalehnovi, Comparison of various machine learning algorithms used for compressive strength prediction of steel fiber-reinforced concrete, Sci. Rep. 13 (1) (Dec. 2023), https://doi.org/10.1038/s41598-023-30606-y.
[85] M. Shang, et al., Predicting the mechanical properties of RCA-based concrete using supervised machine learning algorithms, Materials 15 (2) (Jan. 2022), https://doi.org/10.3390/ma15020647.
[86] Y. Cai, et al., A review of monitoring, calculation, and simulation methods for ground subsidence induced by coal mining, International Journal of Coal Science & Technology 10 (1) (Jun. 2023) 1–23, https://doi.org/10.1007/S40789-023-00595-4, 2023 10:1.
[87] J. De-Prado-gil, C. Palencia, P. Jagadesh, R. Martínez-García, A comparison of machine learning tools that model the splitting tensile strength of self-compacting recycled aggregate concrete, Materials 15 (12) (Jun. 2022), https://doi.org/10.3390/ma15124164.
[88] P. Saha, M.L.V. Prasad, P. RathishKumar, Predicting strength of SCC using artificial neural network and multivariable regression analysis, Comput. Concr. 20 (1) (Jul. 2017) 31–38, https://doi.org/10.12989/cac.2017.20.1.031.
[89] D. Zheng, et al., Flexural strength prediction of steel fiber-reinforced concrete using artificial intelligence, Materials 15 (15) (Aug. 2022), https://doi.org/10.3390/ma15155194.
[90] A. Ahmad, K.A. Ostrowski, M. Maślak, F. Farooq, I. Mehmood, A. Nafees, Comparative study of supervised machine learning algorithms for predicting the compressive strength of concrete at high temperature, Materials 14 (15) (Aug. 2021), https://doi.org/10.3390/ma14154222.